Mean Regional Cerebral Blood Flow Images of Normal Subjects Using Technetium-99m-HMPAO by Automated Image Registration

Muhammad Babar Imran, Ryuta Kawashima, Kazunori Sato, Shigeo Kinomura, Hiroshi Ito, Masamichi Koyama, Ryoi Goto, Shuichi Ono, Seiro Yoshioka and Hiroshi Fukuda

Department of Nuclear Medicine and Radiology, Division of Brain Sciences, Institute of Development, Aging and Cancer, Tohoku University, Sendai, Japan

The purpose of this study was twofold: to calculate relative uptake values for ^{99m}Tc-HMPAO in various regions of the normal brain after alignment and registration to a standard shape and size, and to validate the automated image registration (AIR) program for SPECT-to-SPECT transformation. **Methods:** Thirty subjects took part in this study. Technetium-99m-HMPAO brain SPECT and x-ray–CT scans were acquired. SPECT images were normalized to an average activity of 100 counts/pixel. Intersubject accuracy was evaluated on brain images of 17 normal subjects (mean age = 64.9 ± 8.7 yr). These images were aligned and registered to a standard size and shape with the help of AIR. Realigned images were overlaid on reference images to determine the overlap areas. Intrasubject accuracy was evaluated by realigning 20° rotated brain images with an index calculated as: overlap area/(overlap area + nonoverlap area). Anatomical variability between realigned target and reference images was evaluated by measurements on corresponding x-ray–CT scans, realigned using transformations that were established by the SPECT images. Realigned brain SPECT images of 30 normal subjects (mean age = 50.7 ± 18.7 yr), including those subjects examined in the accuracy validation study, were used to generate mean and s.d. images. Images based on the mean value of each voxel (n = 30) were compared with other mean images prepared by the human brain atlas (HBA) standardization technique on a voxel-by-voxel basis to generate T maps. **Results:** Accuracy indices were 0.98 ± 0.006 and 0.99 ± 0.002 for the intersubject and intrasubject evaluations, respectively. The maximum anatomical variability was 4.7 mm after realignment. Paired Student's t-test comparisons of mean HBA and AIR images revealed statistically significant differences for the deep white matter, pons and occipito-temporal regions. These differences could be explained by variation in the population being studied and the protocol for data handling by AIR and HBA. **Conclusion:** AIR aligns and registers brain SPECT images with acceptable accuracy, without the necessity of MRI or x-ray–CT scans.

Key Words: regional cerebral blood flow; HMPAO brain SPECT; automated image registration; image alignment

J Nucl Med 1998; 39:203–207

Studies of regional cerebral blood flow (rCBF) with SPECT provide valuable functional and biochemical insights into the normal and pathological states of the brain (*1*). In many instances, comparison of successive rCBF measurements in the same subject allows the elucidation of the natural history of the disease or the effect of a particular variable (*2*). Intersubject comparisons can be used to determine the differences in rCBF patterns between diseases and normal variations (*3*). However, individual rCBF images have limited geometrical resolution, and potential discrepancies may occur in positioning between successive imagings. Moreover, individual rCBF image patterns acquired by radiotracer uptake studies vary from one subject to another, and so it is more appropriate to aim for group comparisons to reduce anatomical and radioisotope uptake variance (*4,5*). The generation of mean rCBF images for similar groups of subjects requires aligning and registering individual rCBF images to the specific size and shape of a standard (*6,7*). Objective methods for image alignment and registration are, therefore, very important (*8*).

There have been several approaches to aligning tomographic images, including manual alignment and the derivation of transformation matrices between images, based on their edge location in combination with other fiducial markers (*9*) or based on area-related parameters and image correlation methods (*10,11*). These vary in their reproducibility and accuracy, depending on the amount of information used in computing the transformation matrix.

Automated image registration (AIR) is a program, recently developed by Woods et al. (*12*), that realigns and registers any brain image with respect to another specified reference image. Registration parameters are computed, taking only functional data, i.e., voxel-based information, into account. Basically, the method calculates the ratio between the test and the reference image, voxel by voxel, within the brain. Then, the mean value of this ratio over all pixels and the s.d. from this mean are calculated. The criterion for a good registration is minimization of the s.d. divided by the mean. An arbitrary normalization constant is sought, and the minimum is found in an iterative manner (*12,13*). The software, however, has not yet been validated for intersubject SPECT images. We evaluated the accuracy of AIR for intersubject and intrasubject registration of SPECT brain HMPAO images. A mean image was generated by fitting brain SPECT images of normal subjects and compared with that obtained in another study using the human brain atlas (HBA) standardization procedure (*14*). The latter requires anatomical images and is operator-dependent, whereas AIR does not require such images and is operator-independent.

MATERIALS AND METHODS

All subjects who participated in this study were right-handed by H.N. handedness inventory, and none had any previous signs or symptoms that could affect rCBF studies. All subjects had a normal x-ray–CT scan, taken immediately after SPECT measurements. Written informed consent was obtained from each subject, according to the Declaration of Human Rights of Helsinki, 1975. Each SPECT scan was performed 10 min after an intravenous bolus injection of 1036–1110 MBq ^{99m}Tc-HMPAO, with the subject lying in the supine position with eyes closed during the injection and acquisition periods (approximately 25 min). A SPECT scanner

Received Nov. 25, 1996; revision accepted Mar. 19, 1997.

For correspondence or reprints contact: Muhammad Babar Imran, MBBS, MS, Department of Nuclear Medicine and Radiology, Division of Brain Sciences, Institute of Development, Aging and Cancer, Tohoku University, 4-1, Seiryo machi, Aoba-ku, Sendai, Japan 980-77.

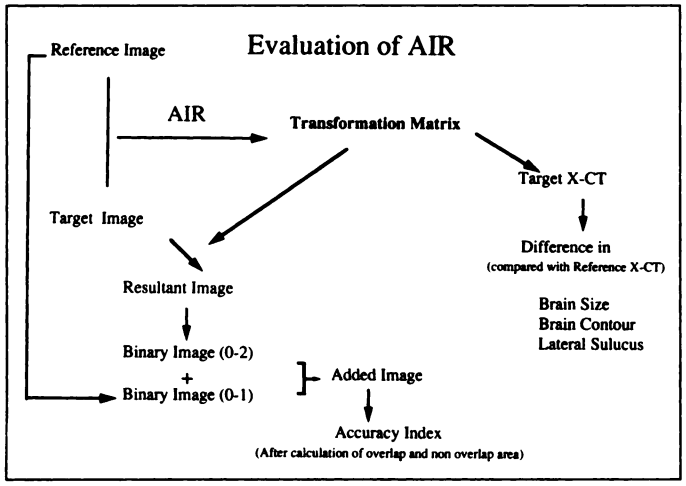

FIGURE 1. Flow chart to evaluate AIR accuracy for brain SPECT studies.

(SPECT-2000H; Hitachi Medico Corp., Tokyo, Japan) (*15*), four-head rotating camera with in-plane and axial resolution of 8 mm FWHM, fitted with low-energy, high-resolution collimators, was used for all measurements. Image reconstruction was performed by filtered backprojection using a Butterworth filter (dimension = 12; cutoff = 0.25 cycle/pixel). Attenuation correction was made numerically by assuming the object shape to be an ellipse for each slice and the attenuation coefficient to be uniform (0.1/cm). Correction for scatter photons was not performed. Image slices were set up parallel to the canthomeatal line and obtained at 8-mm intervals through the brain. After SPECT measurements, x-ray–CT scans were obtained with the same canthomeatal line as that applied for SPECT in all subjects. All reconstructed images were transferred to a Unix workstation for further analysis.

Intersubject Validity of AIR for SPECT Images

Seventeen normal subjects with a mean age of 64.9 ± 8.7 yr (range = 49–81 yr) participated in this part of the study. SPECT images were globally normalized by averaging whole-brain radioactivity to 100 counts/pixel (referred to as normalization). The SPECT image of each subject was realigned with respect to one specific image using AIR. The brain SPECT image of Subject 1 in the study was taken arbitrarily as a reference image for alignment to evaluate the accuracy of AIR, with the intention of calculating actual variance in anatomical structures on corresponding x-ray–CT scans of subjects.

SPECT images were converted into binary images. In the reference image, the brain and nonbrain areas were assigned values 1 and 0, respectively, with 20% of the maximum pixel value set as the threshold. In the target image, the respective values were 2 and 0, with the same set threshold. Reference and target images were added to calculate overlap area, having a value of 3, and nonoverlap areas, having a value of 1 or 2. The ratio of the overlap to nonoverlap areas gives the accuracy index (AI) as:

$$AI = \text{Overlap area}/(\text{Overlap area} + \text{Nonoverlap area}).$$

Using the same transformation matrix as that for SPECT-to-SPECT realignment, x-ray–CT scans were realigned. The x-ray–CT scan of the reference subject and the realigned x-ray–CT scans of all subjects were displayed in a Talairach grid. Variance in size, maximum discrepancy in contours between each target subject and the reference (at three horizontal sections: −10, 0 and +10, on the Talairach grid) and the medial and lateral openings of lateral sulci were noted in the x (side to side of brain) and y (anteroposterior) planes on transverse slices. Diagonal distances for each point were calculated using the formula reported previously (*3*):

$$\text{Diagonal distance} = \sqrt{\Delta x^2 - \Delta y^2}.$$

Intrasubject Validity of AIR for SPECT Images

The intrasubject realignment and registration accuracy of AIR was evaluated for the brain SPECT images of all subjects (n = 17) used in the intersubject validity process. Individual images were rotated 20° clockwise in the sagittal plane, with respect to the original images, and then were registered by AIR with reference to the original images. An accuracy index was calculated for each subject, as detailed above (Fig. 1).

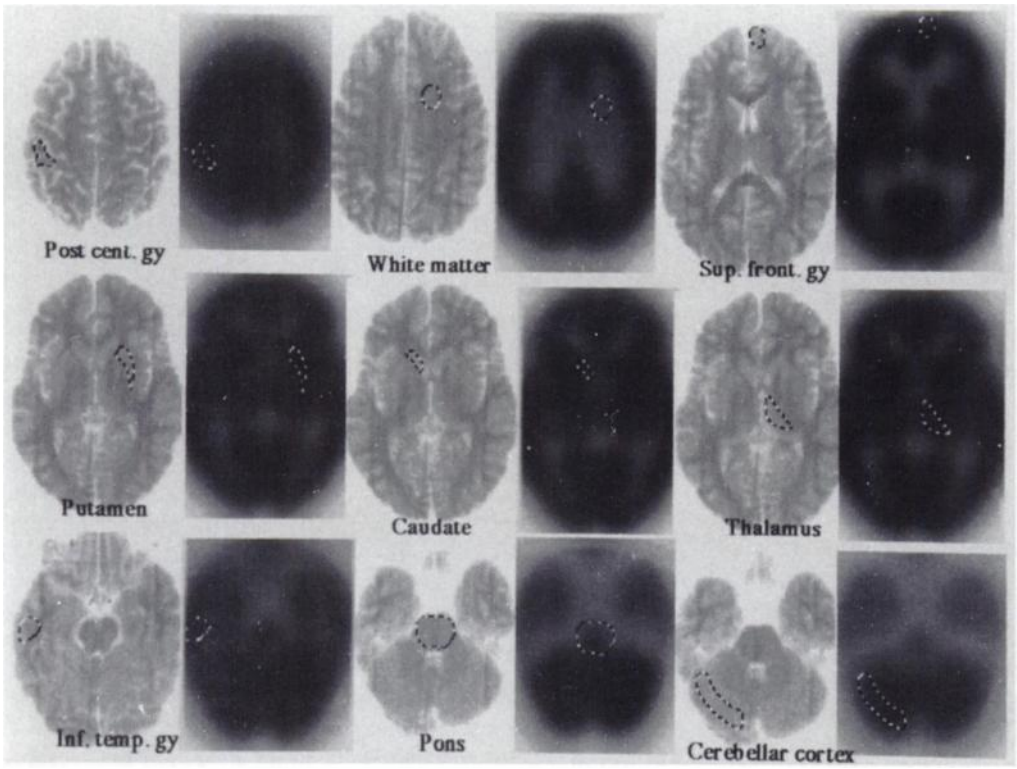

FIGURE 2. Manual drawings of ROIs on MRI and displays on corresponding SPECT slices.

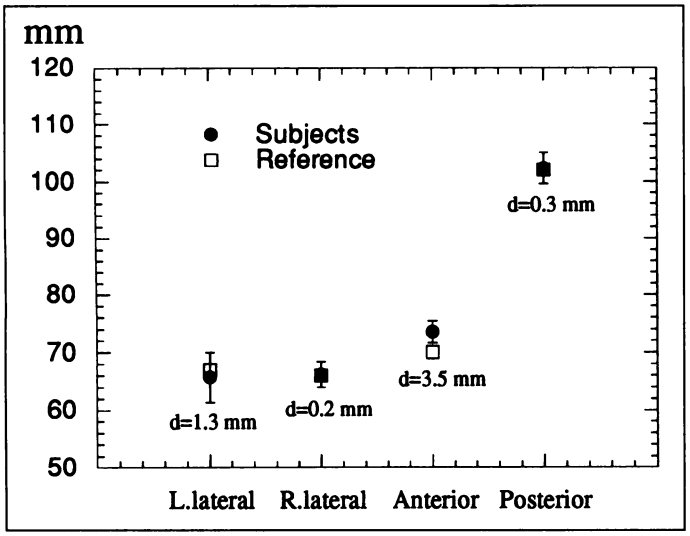

FIGURE 3. Brain size evaluated on transverse slice at 0 mm of a Talairach grid. The distance from the origin of the grid (0,0) to the edge of the brain in the direction shown was plotted. L and R = left and right, respectively; d = difference between the subjects' mean value and reference.

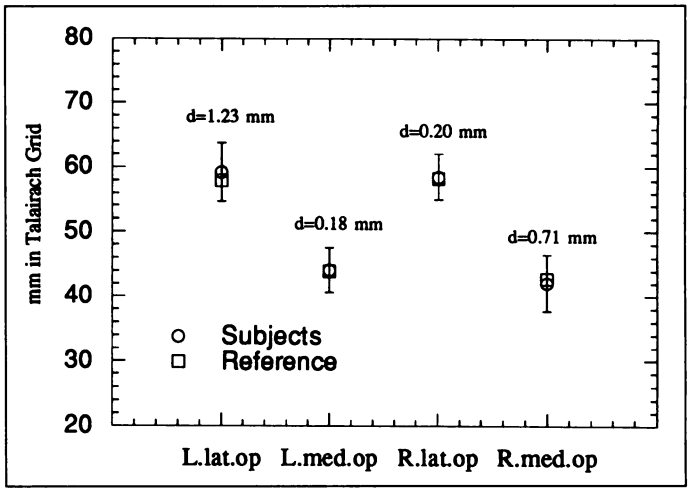

FIGURE 5. Positions of lateral sulci (medial and lateral openings), determined by x-ray–CT scans, of 17 subjects and the reference subject shown in Talairach grid. d = difference between the target subjects and the reference.

Mean Image Generation

Thirty normal subjects with a mean age of 50.7 ± 18.7 yr (range = 20–81 yr) participated in this part of the study, including the 17 subjects whose brain SPECT images were used for evaluating AIR accuracy. After normalization, all SPECT images were registered, with respect to the standard image, to give a similar size and shape. The mean HMPAO-SPECT image of 18 normal subjects obtained in another study in this institute, using the HBA was taken as standard (*16*). Therefore, after realignment by AIR, each subject image was transformed into the same size and shape of the standard brain of the HBA system. Then, mean and s.d. images were calculated on a voxel-by-voxel basis after smoothing with a 10-mm three-dimensional filter. Regions of interest (ROIs) for anatomical structures, shown in Figure 2, were manually drawn, as reported previously (*14*), on standard brain MRIs of the HBA and then displayed on the corresponding slices of the SPECT image of each subject. The mean and s.d. values for the relative radioisotope (RI) concentrations were calculated for each region. Bilateral asymmetry was evaluated by the asymmetric index as:

$$\text{Asymmetric index} = \frac{L - R}{L + R} \times 100,$$

where L and R represent counts on left and right sides, respectively. Asymmetry was considered to be significant when the index value was above 5 (*17*).

The mean rCBF (AIR) was statistically compared with the mean rCBF (HBA), voxel by voxel. The two-sample Student's t-test was applied to calculate a "t" value for each pixel. These t values were displayed as color codes in corresponding pixels to generate a three-dimensional T map. Values over 2.1 were regarded as statistically significant, corresponding to a significance level of $p < 0.05$, as reported previously (*18*).

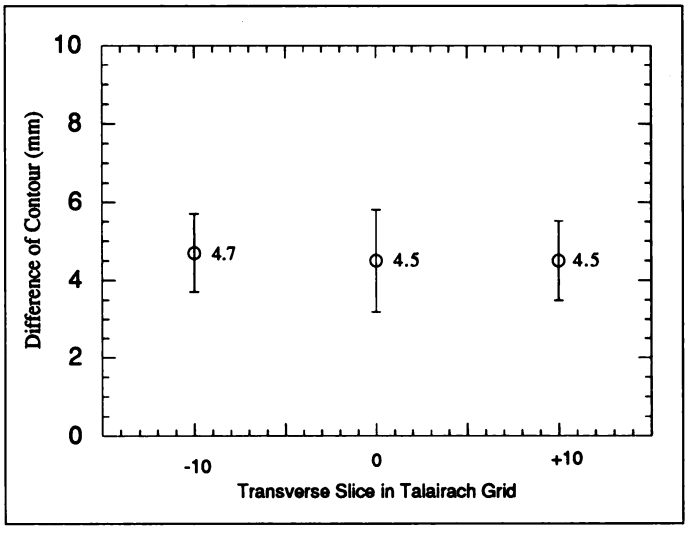

FIGURE 4. Contour differences (means and s.d.) of target and reference subjects, determined by x-ray–CT scan and shown at −10, 0 and +10 mm of a Talairach grid.

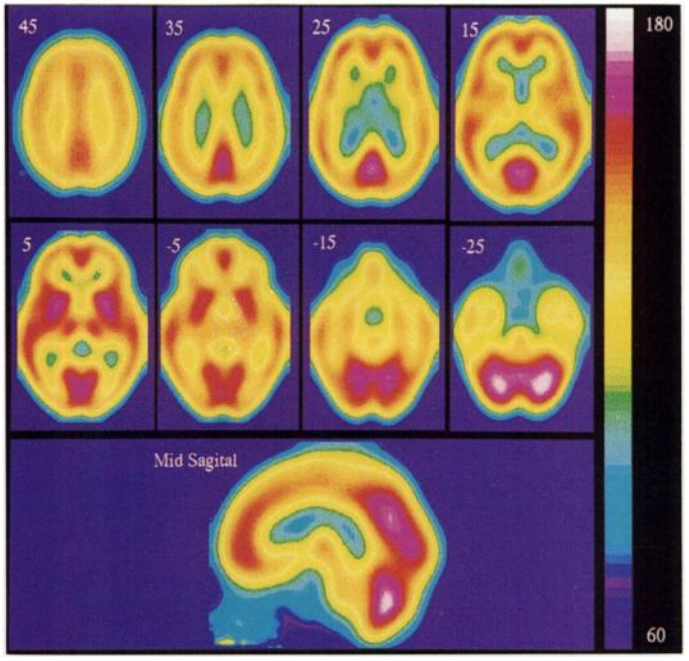

FIGURE 6. Mean of realigned ^{99m}Tc-HMPAO SPECT images. The mean global value is 100 counts/pixel. All slices, except that at the bottom, are parallel to the horizontal plane through the intercommissural line (the top left image is 45 mm above the intercommissural line, and the following pictures were taken at 10-mm intervals). The anterior is on the top of the image, and the subject's right is on the left. The mid-sagittal section is shown at the bottom.

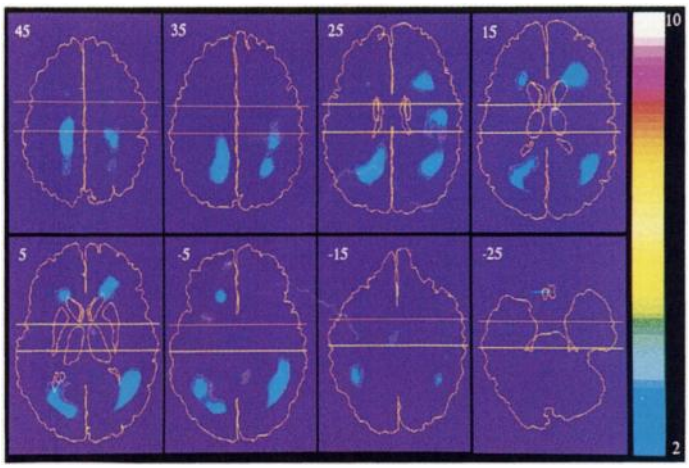

FIGURE 7. Two paired Student's t-test values (mean image of AIR − mean image of HBA), displayed as color codes on the corresponding pixels of brain image. The threshold setting is at 2.1, corresponding to a significance level of $p < 0.05$. The slice location is the same as that for Figure 6.

RESULTS

Accuracy indices from the intersubject and intrasubject evaluations were calculated to be 0.98 ± 0.006 and 0.99 ± 0.002, respectively. Figures 3–5 show variations (anatomical variance as noted on realigned structural images) in brain size, contours and positions of the medial and lateral openings of the lateral sulci. The range was from 0.18 mm to 4.7 mm. These results show little inaccuracy in terms of anatomical variance, but the maximum value is still below the resolution of the gamma camera.

Figure 6 shows mean rCBF SPECT images, and Figure 7 shows a T map, displaying the "t" values of corresponding voxels, according to the color scale shown on the side. There is concordance between the RI values for the cortical regions. However, deep white matter, pons and occipito-temporal regions show high "t" values (over 2.1), demonstrating significant differences between the two images ($p < 0.05$).

Table 1 summarizes ROI data for HMPAO relative counts per pixel in various regions, as well as asymmetric indices for these regions. Bilateral asymmetry is not statistically significant and is far below the limit of significance reported previously ($p < 0.1$) (*17*)

DISCUSSION

The AIR program can align and register brain images obtained with different modalities based on voxel data, thus allowing generation of a mean image from aligned brain images of sample subjects of a population. This program already has been validated for PET and MRI registration, but its applicability for SPECT-to-SPECT transformations has not been tested.

TABLE 1
HMPAO Counts in Various Regions of the Brain by ROI Method

Region	HMPAO (counts/voxel)			Asymmetric index
		Left hemisphere	Right hemisphere	
Brain stem				
Pons	103.95 ± 7.64			
Midbrain	116.22 ± 6.21			
Cerebellum		144.66 ± 7.66	140.56 ± 6.17	1.76 ± 1.41
Vermis	145.57 ± 6.79			
Basal ganglia				
Caudate nucleus		126.92 ± 8.28	128.75 ± 7.59	1.40 ± 0.97
Putamen		143.12 ± 5.93	143.80 ± 5.15	0.90 ± 0.74
Thalamus limbic system		128.21 ± 5.67	128.66 ± 5.55	0.83 ± 0.61
Anterior cingulate gyrus		127.06 ± 8.71	126.04 ± 8.09	1.13 ± 0.86
Parahippocampus		117.21 ± 7.15	117.63 ± 6.83	1.10 ± 0.71
Temporal cortex				
Superior temporal gyrus		127.75 ± 9.00	129.94 ± 8.04	1.34 ± 0.91
Mid temporal gyrus		126.02 ± 5.45	129.52 ± 4.25	1.72 ± 1.17
Inferior temporal gyrus		120.32 ± 6.35	122.31 ± 5.92	1.31 ± 0.97
Insular cortex, frontal cortex		131.92 ± 8.16	134.34 ± 8.28	1.22 ± 0.96
Superior frontal gyrus		122.33 ± 7.19	124.16 ± 6.65	1.06 ± 0.82
Mid frontal gyrus		122.14 ± 5.83	123.75 ± 5.42	1.33 ± 0.97
Inferior frontal gyrus		121.72 ± 7.56	122.65 ± 7.27	1.22 ± 0.80
Precentral gyrus		119.89 ± 5.15	120.45 ± 5.38	1.05 ± 0.91
Parietal cortex				
Post central gyrus		118.89 ± 6.03	117.34 ± 6.25	1.16 ± 0.90
Precuneus		141.06 ± 8.52	138.51 ± 8.77	1.33 ± 1.01
Occipital cortex				
Lingual gyrus		140.17 ± 5.75	139.32 ± 6.72	0.91 ± 0.73
Cuneus		137.82 ± 7.28	136.93 ± 6.49	1.20 ± 0.81
Posterior occipital area		120.77 ± 9.55	120.33 ± 8.27	1.35 ± 1.02
Lateral occipital area		114.95 ± 5.47	114.94 ± 6.04	1.12 ± 0.77
White matter				
Anterior periventricular white matter		93.29 ± 4.99	93.75 ± 4.53	1.09 ± 0.83
Posterior periventricular white matter		86.95 ± 6.42	88.88 ± 5.68	2.03 ± 1.58
Centrum semi ovale		93.93 ± 4.60	95.48 ± 4.87	1.60 ± 1.24

The observed inaccuracies (1.0 − accuracy index) of only 0.02 and 0.01, on average, upon evaluation of intersubject and intrasubject alignments, respectively, are low. The error in terms of anatomical landmarks measured by x-ray–CT scans was a maximum of 4.7 mm, which is comparable with a previous study in which structural images were used for transformation and the s.d. of anatomical variance was approximately 4.5 mm (*19*). When a transformation matrix of SPECT alignment is applied to respective x-ray–CT scans, there is always a propagation error, in addition to errors in positioning and acquisition. However, the maximum error still proved to be below the resolution of the gamma camera (8 mm FWHM). Therefore, it can be considered within acceptable limits (*1,20*). Here, we used ^{99m}Tc-HMPAO because it is one of the most commonly used radiopharmaceuticals for rCBF imaging (*21,22*). The mean image can be used for future reference because it reduces individual variance and facilitates differentiation of significant from nonsignificant variation in radioisotope uptake (*23*). It is particularly important for objective comparisons of normal subjects with disease cases (*6,18*). The mean image obtained in this study showed a distribution that was similar to that of the mean image generated by the HBA anatomical standardization technique (*16*). However, statistically significant differences in radioisotope counts were found for the deep white matter in the periventricular region, pons and occipito-temporal regions. This might have been due to differences in the study populations because age affects the appearance of brain images (*24*). We used a general population with an age range of 20–81 yr, whereas the HBA study was performed for a sample containing relatively young subjects. Another reason might be that the HBA uses structural information only, whereas AIR uses voxel data, including counts per voxel.

Being a noninteractive, fully automated program, AIR, like other automated programs, cannot be expected to be absolutely perfect, and accuracy is always slightly less than 100%. When data from different subjects are transformed using the 12-parameter affine model, there might be some partial-volume averaging effects. However, these artifacts must be very small; this problem has been addressed by Kinomura et al. (*25*). Moreover, AIR uses global fitting and linear parameters. This might have been one cause for the significantly high "t" values found in the T map, but this kind of artifact is not important when intersubject or intrasubject comparisons are performed using AIR for alignment.

CONCLUSION

Automated image registration can transform intersubject and intrasubject SPECT brain images with acceptable accuracy and reproducibility. Using identical parameters, multicenter and group studies easily can be performed. The generation of group mean images for normal subjects of different age and sex groups should help to ascertain normal radiopharmaceutical distribution, with reduced individual and anatomical variance. Automated comparisons and auto report generation by comparing the group mean of normal subjects with aligned patient images are facilitated by AIR.

ACKNOWLEDGMENTS

This study was supported by a grant-in-aid for scientific research from Telecommunications Advancement Organization and fund for comprehensive research on aging and health from the Ministry of Health and Welfare, Japan. Muhammad Babar Imran is an S & T scholar, financially supported by the Ministry of Science and Technology, Pakistan. We thank the staff of the Institute of Development, Aging and Cancer, Tohoku University, and, in particular, Tachio Sato for his technical help acquiring SPECT images.

REFERENCES

1. Stollberger R, Fazekas F, Payer F, Flooh E. Morphology oriented analysis of cerebral SPET using matched magnetic resonance images. *Nucl Med Commun* 1995;16:265–272.
2. Talacchi A. Sequential measurements of cerebral blood flow in the acute phase of subarachnoid haemmorrhage. *J Neurosurg Sci* 1993;37:9–18.
3. Eberl S, Kanno I, Fulton RR, Ryan A, Hutton BF, Fulham MJ. Automated interstudy image registration technique for SPECT and PET. *J Nucl Med* 1996;37:137–145.
4. Minoshima S, Kieppe RA, Fery KA, Ishihara M, Kuhl DE. Stereotactic PET atlas of the human brain: aid for visual interpretation of functional brain images. *J Nucl Med* 1994;35:949–954.
5. Minoshima S, Kieppe RA, Fery KA, Kuhl DE. Anatomic standardization: linear scaling and nonlinear warping of functional brain images. *J Nucl Med* 1994;35:1528–1537.
6. Houston AS, Kemp PM, Macleod MA. A method for assessing the significance of abnormalities in HMPAO brain SPECT images. *J Nucl Med* 1994;35:239–244.
7. Links JM. The influence of positioning and accuracy and precision in emission tomography. *J Nucl Med* 1991;32:1252–1253.
8. Habboush IH, Mitchell KD, Mulern RV, Barnes PD, Treves ST. Registration and alignment of three-dimensional images: an interactive visual approach. *Radiology* 1996;199:573–578.
9. Evans A, Beil C, Marret C, Thompson C, Hakim A. Anatomical functional correlation using an adjustable MRI based ROI atlas with positron emission tomography. *J Cereb Blood Flow Metab* 1988;8:513–530.
10. Alpert N, Bradshaw J, Senda M, Correia J. The principal axis transformation: a method for image registration. *J Nucl Med* 1989;30:776.
11. Junck L, Moen JG, Hutchins GD, Brown MB, Kuhl DE. Correlation methods for centering, rotating, and alignment of functional brain images. *J Nucl Med* 1990;31:1220–1226.
12. Woods RP, Cherry SR, Mazziotta JC. Rapid automated algorithm for aligning and reslicing PET images. *J Comput Assist Tomogr* 1992;16:620–633.
13. Woods RP, Mazziotta JC Cherry SR. MRI-PET registration with automated algorithm. *J Comput Assist Tomogr* 1993;17:536–546.
14. Koyama M, Kawashima R, Ito H, et al. SPECT images with technetium-99m-HMPAO and technetium-99m-ECD in normal subjects. *J Nucl Med* 1997;38:587–592.
15. Kimura K, Hashikawa K, Wtani H, et al. A new apparatus for brain imaging: four head rotating gamma single photon emission computed tomography. *J Nucl Med* 1990;31:603–609.
16. Koyama M, Kawashima R, Ito H, et al. Normal cerebral perfusion of Tc-99m HMPAO brain SPECT: evaluation by an anatomical standardization technique. *Jpn J Nucl Med* 1995;32:967–977.
17. Poderka I, Suess E, Goldenberg G, et al. Initial experience with technetium-99m-HMPAO brain SPECT. *J Nucl Med* 1987;28:1657–1666.
18. Ito H, Kawashima R, Awata S, et al. Hypoperfusion in the limbic system and prefrontal cortex in depression: SPECT with anatomic standardization technique. *J Nucl Med* 1996;37:410–414.
19. Roland PE, Graufelds CJ, Wahlin J, et al. Human brain atlas: high resolution functional and anatomical mapping. *Hum Brain Mapping* 1994;1:173–184.
20. Verra P, Farman-Ara B, Stievenart JL, et al. Proportional anatomical stereotactic atlas for visual interpretation of brain SPECT perfusion images. *Eur J Nucl Med* 1996;23:871–877.
21. Smith FW, Besson JAO, Gemmell HG, Sharp PF. The use of technetium-99m HMPAO in the assessment of patients with dementia and other neuropsychiatric conditions. *J Cereb Blood Flow Metab* 1988;8(suppl):S116–S122.
22. Matsuda H, Tsuji S, Shuke N, Sumiya H, Tonami N, Hisada K. A quantitative approach to technetium-99m-hexamethylpropylene amine oxime. *Eur J Nucl Med* 1992;19:195–200.
23. Fox PT, Mintun MA, Reiman ER, Raichle ME. Enhanced detection of focal brain responses using intersubject averaging and change distribution analysis of subtracted PET images. *J Cereb Blood Flow Metab* 1988;8:642–653.
24. Matsuda H, Tsuji S, Shuke N, Sumiya H, Tonami N, Hisada K. Noninvasive measurements of regional cerebral blood flow using technetium-99m-hexamethylpropylene amine oxime. *J Nucl Med* 1993;20:391–401.
25. Kinomura S, Kawashima R, Sato K, Kinomura S Imran MB, Fukuda H. Intersubject transformation of brain SPECT by automated image registration (AIR): effects of defects in the target image [Abstract]. *Ann Nucl Med* 1996;10(suppl):s222.